Bioorganic & Medicinal Chemistry 26 (2018) 1092–1101

Contents lists available at ScienceDirect

Bioorganic & Medicinal Chemistry

journal homepage: www.elsevier.com/locate/bmc

Synthesis and activity evaluation of a series of cholanamides as modulators of the liver X receptors

Mario D. Martínez [a,c], Alberto A. Ghini [a,c], M. Virginia Dansey [b,c], Adriana S. Veleiro [a,c], Adali Pecci [b,d], Lautaro D. Alvarez [a,c], Gerardo Burton [a,c,*]

[a] Universidad de Buenos Aires, Facultad de Ciencias Exactas y Naturales, Departamento de Química Orgánica, Buenos Aires, Argentina
[b] Universidad de Buenos Aires, Facultad de Ciencias Exactas y Naturales, Departamento de Química Biológica, Buenos Aires, Argentina
[c] CONICET – Universidad de Buenos Aires, UMYMFOR, Buenos Aires, Argentina
[d] CONICET – Universidad de Buenos Aires, IFIBYNE, Buenos Aires, Argentina

ARTICLE INFO

Article history:
Received 28 November 2017
Revised 18 January 2018
Accepted 26 January 2018
Available online 31 January 2018

Keywords:
Liver X receptors
Steroid amides
Molecular dynamics
DMHCA

ABSTRACT

The Liver X receptors (LXRs) are members of the nuclear receptor family, that play fundamental roles in cholesterol transport, lipid metabolism and modulation of inflammatory responses. In recent years, the synthetic steroid *N*,*N*-dimethyl-3β-hydroxycholenamide (DMHCA) arised as a promising LXR ligand. This compound was able to dissociate certain beneficial LXRs effects from those undesirable ones involved in triglyceride metabolism. Here, we synthetized a series of DMHCA analogues with different modifications in the steroidal nucleus involving the A/B ring fusion, that generate changes in the overall conformation of the steroid. The LXRα and LXRβ activity of these analogues was evaluated by using a luciferase reporter assay in BHK21 cells. Compounds were tested in both the agonist and antagonist modes. Results indicated that the agonist/antagonist profile is dependent on the steroid configuration at the A/B ring junction. Notably, in contrast to DMHCA, the amide derived from lithocholic acid (**2**) with an A/B cis configuration and its 6,19-epoxy analogue **4** behaved as LXRα selective agonists, while the 2,19-epoxy analogues with an A/B trans configuration were antagonists of both isoforms. The binding mode of the analogues to both LXR isoforms was assessed by using 50 ns molecular dynamics (MD) simulations. Results revealed conformational differences between LXRα- and LXRβ-ligand complexes, mainly in the hydrogen bonding network that involves the C-3 hydroxyl. Overall, these results indicate that the synthetized DMHCA analogues could be interesting candidates for a therapeutic modulation of the LXRs.

1. Introduction

The liver X receptors (LXRs) are established mediators of lipid-inducible gene expression and their activation regulates important steps in cholesterol, fatty acid and bile acid metabolism.[1–3] There are two isoforms of the LXRs, LXRα and LXRβ. LXRα expression predominates in metabolically active tissues such as liver, small intestine, kidney, macrophages and adipose tissue, whereas LXRβ is more ubiquitously expressed with particular high levels in the brain. Many potential applications targeting LXRs have been proposed for the treatment of several diseases such as atherosclerosis, type 2 diabetes and Alzheimer disease.[4–6] However, LXR agonists elevate liver triglycerides by increasing transcriptional levels of genes that regulate lipogenesis, such as sterol regulatory element binding transcription factor 1 (SREBP-1c) and fatty acid synthase (FAS), leading to hepatotoxicity.[7] Thus development of therapeutically useful LXR agonists may require a separation of favorable effects on cholesterol reverse transport from the unfavorable effects on triglyceride metabolism. One approach to achieve this goal takes advantage of the predominant expression of the LXRα isoform in the liver, by designing selective agonists for the β isoform that should have a reduced effect on elevating liver triglycerides. However, activation of LXRα in macrophages is required for reduction of atherosclerotic plaques and for cholesterol efflux.[3] An alternate approach seeks selectivity through differential gene regulation probably associated with selective recruitment of specific coactivators or corepressors.[8] Thus LXR subtype-specific ligands and novel ligands that possess tissue-specific agonist/antagonist properties might provide drug candidates with improved therapeutic profiles.

The endogenous LXR ligands are cholesterol metabolites that include additional oxidized moieties at the side chain. Examples

* Corresponding author at: Universidad de Buenos Aires, Facultad de Ciencias Exactas y Naturales, Departamento de Química Orgánica, Buenos Aires, Argentina.
E-mail address: burton@qo.fcen.uba.ar (G. Burton).

https://doi.org/10.1016/j.bmc.2018.01.025
0968-0896/

are the 24(*S*),25-epoxycholesterol, 24(*S*)-hydroxycholesterol and 22(*R*)-hydroxycholesterol that are agonists for both LXRs.[9,10] Other oxidized derivatives of cholesterol as 25(*R*)-cholestenoic acid also activate the LXRs.[11] The synthetic ligand *N*,*N*-dimethyl-3β-hydroxycholenamide (DMHCA, **1**) is an agonist of both LXRs that shows tissue and gene-selective differential regulation of the ATP-binding cassette transporter 1 (ABCA1) and SREBP-1c both *in vitro* and *in vivo*.[12] Cell-based studies indicate that DMHCA enhances cholesterol efflux in macrophages without stimulating lipogenesis. This steroidal amide neither increases plasmatic VLDL or LDL-cholesterol nor liver lipid accumulation,[12] and on long-term administration it significantly reduced atheroma formation in apoE-null mice, without increasing the hepatic triglyceride (TG) levels.[13] Moreover, it has been reported that DMHCA exhibits antiinflammatory effects in animal models without inducing liver lipid accumulation or liver injury.[14]

Recently, we reported that the removal of the C-25 methyl group of cholestenoic acid, gives rise to a drastic change from agonism to inverse agonism in the LXRs response and proposed that this change may originate in conformational differences of the steroid side chain that affect coactivator and corepressor recruitment, by interfering with the anchoring of helix 12 in the agonist conformation.[15] Similar effects have been observed by changing the orientation of substituents on the side chain (e.g. 22R and 22S-hydroxycholesterol).[16] However little is known on the effect of changes of the overall conformation of the steroid nucleus on the LXRs activity profile except that some 3α-hydroxy-5βH steroids are agonists of the LXRs (e.g. hyodesoxycholic acid and a fluorinated analogue).[17] Specifically we were interested in evaluating the effect of changes in the A/B ring fusion and the presence of oxygenated substituents with well defined orientations in that part of the steroid nucleus.

With this purpose we prepared a series of steroidal amides analogues **2**–**6** (Fig. 1), compounds **2**, **3** and **4** present a bent structure at the A/B junction, while compounds **5** and **6** have flat structures at this junction. The rigid compounds **4**–**6** were prepared taking into account that the incorporation of oxygen bridges involving selected atoms of the steroid nucleus provides conformationally restricted analogues that mimic or change in a controlled way the molecular shape of the steroid, and consequently the profile activity. They also act as hydrogen bond acceptors on the β face of the steroid allowing interaction with specific residues in the ligand binding pocket (LBP) of the receptor.

2. Results

2.1. Chemistry

Amides **1**–**3** were prepared from the readily available carboxylic acids and dimethylamine, in the presence of benzotriazol-1-yloxy-tris-(dimethylamino)phosphonium hexafluorophosphate (BOP).[18] Compound **4** was obtained from 3β-acetoxy-5-cholenic acid methyl ester (**7**) as shown in Scheme 1. Introduction of the 6,19-epoxy bridge was carried out by bromohydrin formation followed by photochemical functionalization of C-19 with diacetoxyiodobenzene to give bromoether **8**. Removal of the acetate at C-3 followed by oxidation with pyridinium chlorochromate gave the Δ^4-3-ketone (**9**) that was reduced to the 3α-alcohol **10** with sodium borohydride. Hydrolysis of the methyl ester with lithium hydroxide in methanol followed by acidification gave the carboxylic acid **11** that was reacted with dimethylamine in the presence of BOP to give amide **4**.

Amides **5** and **6** were obtained from bromoether **8** as depicted in Scheme 2. Cleavage of the 6,19-epoxy bridge with zinc/acetic acid gave compound **12**. Acetylation of the 19-hydroxyl, catalytic hydrogenation (H_2, Pd/C 10%, ethyl acetate/ methanol) of the 5,6-double bond followed by regioselective hydrolysis of the 3-acetate in **13** with K_2CO_3 in methanol gave alcohol **14** that was subsequently converted into the Δ^2-steroid **15**. Kumar et al. reported the use of trifluoromethanesulfonic anhydride and dimethylaminopyridine (DMAP) or pyridine as an efficient system for the direct synthesis of various steroidal olefins from the corresponding secondary alcohols.[19] In the case of compound **15** the best results were obtained upon reaction with trifluoromethanesulfonic anhydride in dichloromethane at −20 °C followed by treatment with aqueous sodium acetate, without the addition of an amine. Epoxidation of the 2,3-double bond in **15** with *m*-chloroperbenzoic acid (MCPBA) gave the 2α,3α-epoxy steroid **16**. The stereospecific α-epoxidation of the alkene takes place because the β face of the A ring is sterically hindered due to the presence of the 19-acetate.[20] Deacetylation of **16** with sodium methoxide in methanol resulted in the intramolecular attack of the 19-alcoxide on C-2 to give the 2β,19-epoxy bridge. Hydrolysis of the methyl ester **17** with lithium hydroxide in methanol gave the 2,19-epoxy acid, that was transformed to the corresponding cholanamide **5** as above. The 3β-hydroxy-2,19-epoxy cholanamide **6** was obtained from **5** by oxidation of the 3-hydroxy group with pyridinium chlorochromate followed by reduction of the 3-ketone with $LiAl(t\text{-}BuO)_3H$ in THF.

2.2. Biological evaluation

In order to evaluate whether the amides **2**–**6** were able to modulate the LXRs activities a luciferase reporter assay was performed in BHK21 cells co-transfected with a pRXR together with either the full length human LXRβ or the full length human LXRα expression vectors and the reporter construct pGL3/LRELuc. DMHCA (**1**) was moderately active in this assay increasing basal levels of luciferase activity at 10 μM (Fig. 2a) but was a strong antagonist when co-administered with the synthetic LXR agonist GW3965 (Fig. 2b). Compounds **2** and **4** *per se* selectively increased basal levels of

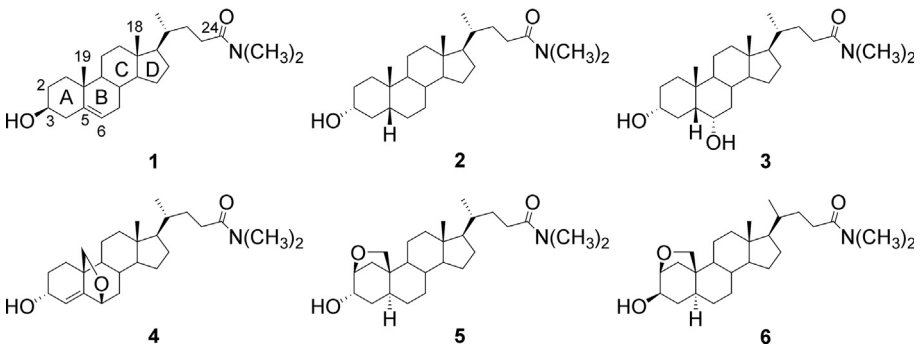

Fig. 1. Structures of DMHCA (**1**) showing numbering of key atoms and analogues **2**–**6**.

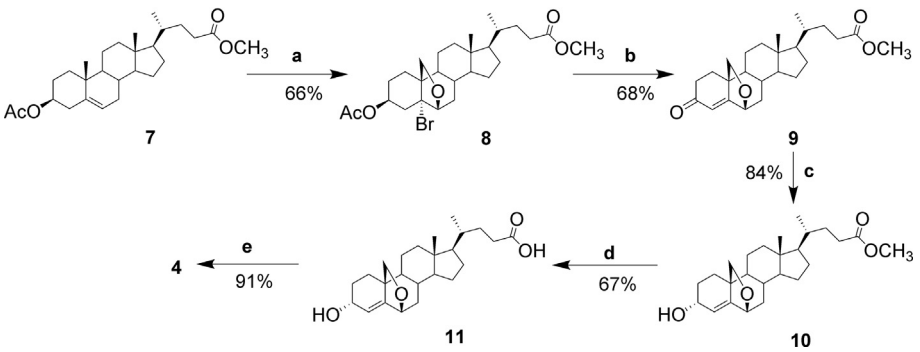

Scheme 1. a) i) 7.5% aqueous perchloric acid, *N*-bromoacetamide, Et_2O-THF, 10 °C, 55 min, ii) DIB, I_2, Cl_2CH_2, h*v*, 25 °C, 30 min; b) i) K_2CO_3/MeOH, THF, 25 °C, 1 h; ii) PCC, $BaCO_3$, 3 Å molecular sieves, Cl_2CH_2, 25 °C, 90 min; c) $NaBH_4$, MeOH-Cl_2CH_2, 25 °C, 40 min; d) aqueous 5% LiOH, THF-MeOH (3:1), 25 °C, 2 h; e) i) (benzotriazol-1-yloxy)-tris (dimethylamino) phosphonium hexafluorophosphate, Cl_2CH_2-DMF, Et_3N, 0 °C 30 min, then 25 °C 2 h, ii) water.

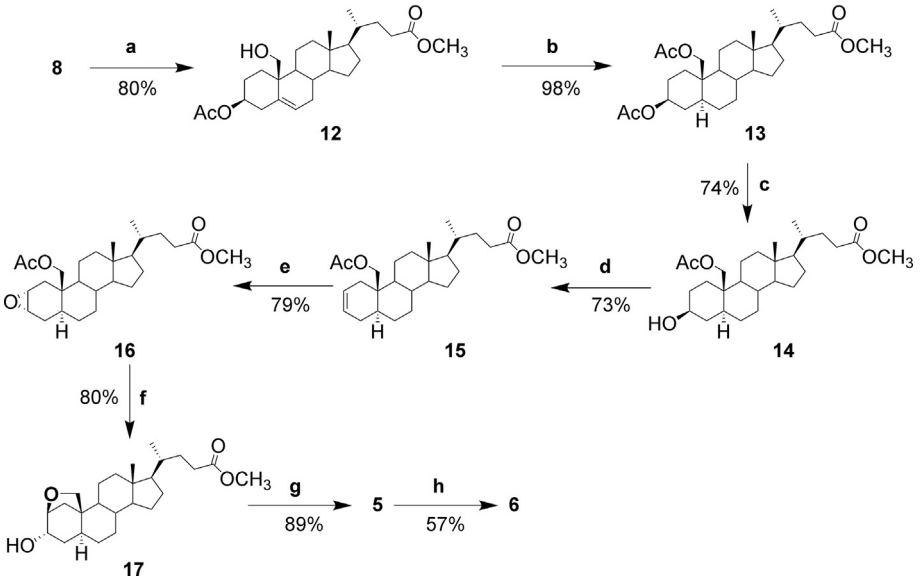

Scheme 2. a) activated Zn, 2-propanol, AcOH, 80 °C, 3 h; b) i) Ac_2O, py, DMAP, Cl_2CH_2, 25 °C, 3 h; ii) H_2, Pd/C 10% w/w, EtOAc-EtOH, 50 psi, 25 °C, 24 h; c) K_2CO_3/MeOH, THF, 25 °C, 1 h; d) i) $(CF_3SO_2)_2O$, Cl_2CH_2, −20 °C, 30 min, ii) sodium acetate, H_2O, 5 min; e) Na_2CO_3/H_2O, MCPBA, Cl_2CH_2, 0 °C 1 h, then 25 °C 2 h; f) NaOMe/MeOH, N_2, 40 °C, 4 h; g) i) aqueous 5% LiOH, THF-MeOH (3:1), 25 °C, 2 h, ii) (benzotriazol-1-yloxy)-tris(dimethylamino)phosphonium hexafluorophosphate, Cl_2CH_2-DMF, Et_3N, 0 °C 30 min, then 25 °C, 2 h, iii) water; h) i) PCC, $BaCO_3$, 3 Å molecular sieves, Cl_2CH_2, 25 °C, 90 min; ii) 1 M lithium tri(*t*-butoxy)aluminum hydride/THF, 0 °C, 2 h (yield based on recovered compound **5**).

luciferase activity at 10 μM (Fig. 2a) mediated by the LXRα isoform, but did not exhibit antagonistic activity (Fig. 2b); for the LXRβ, **2** was a weak agonist while **4** was a weak antagonist. On the other hand, compound **3** significantly increased luciferase activity mediated by LXRβ (Fig. 2a) and behaved as a strong antagonist for both LXR isoforms (Fig. 2b). Compounds **5** and **6** did not affect *per se* luciferase basal levels but exhibited strong antagonism for either receptor isoform (Fig. 2b), revealing pure antagonism for both LXRα and LXRβ.

2.3. Molecular dynamics simulation of LXR/ligand complexes

To gain further insight in the molecular determinants involved in the LXR activity profiles of the steroidal amides **1**–**6**, we studied their ligand binding modes to both isoforms by using 50 ns of molecular dynamics (MD) simulations. In the case of the LXRβ, receptor coordinates of the ligand binding domain (LBD) were taken from the crystal structure of the human LXRβ/24S,25-epoxycholesterol complex (pdb: 1p8d, chain A). Compounds **1**–**6** were directly introduced into the ligand binding pocket (LBP) by superimposing the carbon atoms of C and D rings of optimized structures with the corresponding atoms of 24S,25-epoxycholesterol. In the case of LXRα, since no crystal structures of LXRα/steroid complex has been resolved yet, the starting coordinates of the human LXRα were taken from the crystal structure of the complex with a non steroidal ligand (pdb: 5avi, chain A). Then the backbone atoms of the LXRα and the LXRβ/ligand complexes were superimposed, the ligand coordinates were extracted and combined with the LXRα to obtain the corresponding LXRα/ligand complexes. Visual inspection of LXRα and LXRβ trajectories shows that the global folding remains essentially intact, and the time-dependent residue fluctuation (root-mean square deviations, RMSD) measured over the backbone atoms from the initial structures, reveals that all simulations are reasonably stable (Supplementary material, Fig. S1).

As a first step, we evaluated the LXRα and LXRβ models by determining the ligand binding mode of DMHCA (**1**). The LBDs of LXRα and LXRβ have a 78% of sequence similarity, although residues forming the LBP are the same in both receptors. Our MD results showed that DMHCA (**1**) reached a stable binding in both LXRs. The original position of the steroid is conserved, and polar groups contacted the polar residues of the LBP (Fig. 3a). At the

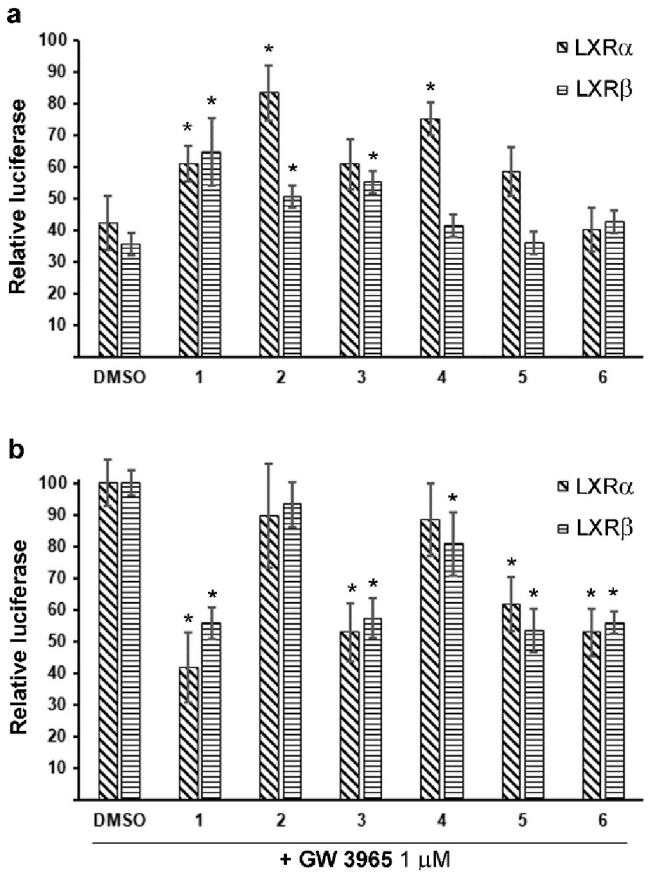

Fig. 2. LXR activity of DMHCA (**1**) and analogues **2**–**6**. Steroids were assayed at 10 μM. Values are expressed as % induction relative to GW3965 1 μM (100%). Means ± S.E. from 3 independent experiments are shown. Differences were determined by one-way ANOVA followed by Dunnett's test. * Significantly different ($p < 0.05$) from their respective control (no steroid added).

steroid side chain, the amide carbonyl forms a strong and persistent hydrogen bond with His421 (LXRα) or His435 (LXRβ). Thus, this group appears to play a role similar to the oxygen atom of the epoxy group of 24S,25-epoxycholesterol, restricting the orientation of this histidine that is crucial to stabilize the agonist conformation of the receptor. At the other end of the steroid molecule, three polar residues around the 3β-hydroxyl take part in a hydrogen bond network, in which water molecules also participate. In the case of LXRβ, the calculation of the hydrogen bond occupancy (HBO) showed that the interaction with the 3β-hydroxyl is similar for the three residues, Asn239, Glu281 and Arg319 (Fig. 3a). Instead, the direct interaction between the ligand and Asn225 and Glu267 was markedly reduced in the LXRα, with the 3β-hydroxyl more exposed to form hydrogen bonds with water molecules (Table 1). Nevertheless, the superposition of representative snapshots of the LXRα/**1** and LXRβ/**1** complexes shows a similar orientation of the four polar residues contacting the ligand (Fig. 4a).

The ligand binding mode of analogues with a bent structure (**2**–**4**) exhibited a similar recognition of the amide group in the steroidal side chain (Fig. 3b–d). However, a marked difference in the interactions with the 3α-hydroxyl group is observed. Thus, because of the overall bent conformation of the steroid nucleus, the 3α-hydroxyl group moves away from Asn225/Asn239 and Arg305/Arg319, while maintaining hydrogen bonds of variable frequency with Glu267/Glu281. In addition, a very persistent interaction is formed between the 3α-hydroxyl and a polar residue (Ser264/Ser278) positioned close to the α face of the steroid. In the case of compounds **3** and **4**, the O6 atom interacts with the backbone atoms of other LBP residues, Phe315/Phe329 and Leu316/Leu330, respectively. These interactions were more frequent in the LXRβ receptor. On the other hand, the calculated HBO between water molecules and the 3α-hydroxyl of these analogues indicates that this ligand group is more accessible for water molecules in the LXRα than in the LXRβ (Table 1).

Thus, when representative snapshots of LXRα/**4** and LXRβ/**4** complexes are superimposed, differences are evident in the conformation (and relative position) of asparagine and glutamic

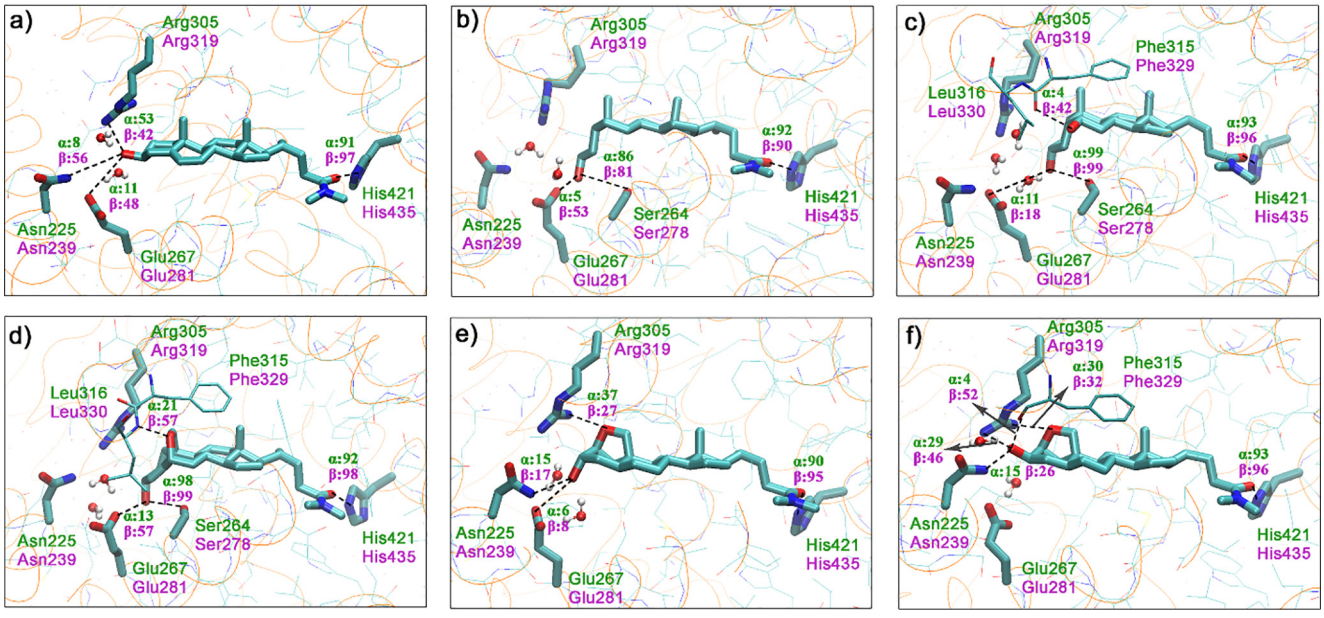

Fig. 3. Binding mode of DMHCA (**1**) and analogues **2**–**6**. Representative snapshots of LXRβ complexed with **1** (a), **2** (b), **3** (c), **4** (d), **5** (e) and **6** (f). Dotted lines indicate a direct hydrogen bond interaction between the ligand and the receptor atoms. Values near the dotted lines are the% Hydrogen Bond Occupancy (HBO) for each interaction (in green for the LXRα and in purple for the LXRβ complexes).

Table 1
Percent Hydrogen Bond Occupancy (HBO) between oxygen atoms of ligands and water molecules in the α and β isoforms of the LXR.[a]

Acceptor	Donor	Compound											
		1		**2**		**3**		**4**		**5**		**6**	
		α	β	α	β	α	β	α	β	α	β	α	β
O3[b]	H_2O	94	82	69	41	91	60	70	20	99	97	93	68
H_2O	O3[b]	69	28	60	14	52	53	15	15	81	82	52	20
O6[b]	H_2O	–	–	–	–	62	53	16	10	–	–	–	–
H_2O	O6[b]	–	–	–	–	52	54	–	–	–	–	–	–

[a] The HBO was calculated using 3.0 Å and 135° for the distance and angle cutoffs respectively.
[b] Ligand Atoms.

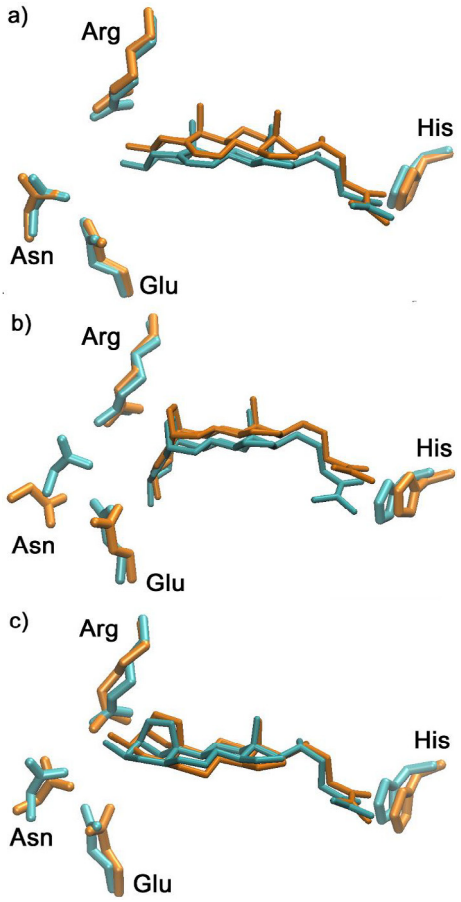

Fig. 4. Superposition of representative snapshots of LXRα (orange) and LXRβ (cyan) complexes with **1** (a), **4** (b) and **6** (c). Arg: Arg305 (LXRα) or Arg319 (LXRβ); Asn: Asn225 (LXRα) or Asn239 (LXRβ); Glu: Glu267 (LXRα) or Glu281 (LXRβ) and His: His421 (LXRα) or His435 (LXRβ).

acid residues (Fig. 4b) and could explain the observed selectivity towards the α isoform. The introduction of an equatorial hydroxyl at C-6 in compound **3**, attenuates the above differences in the interactions with both isoforms (Fig. 3c, Table 1) and in the activity profile which resembles that of DMHCA (Fig. 2).

As in the case of the torsioned analogues (**2**–**4**), the amide carbonyl of the analogues with a flat conformation (**5** and **6**), also forms a strong and very frequent hydrogen bond with the His421/His435 (Fig. 3e,f). However, while the 3α-hydroxyl group of compound **5** only interacts sporadically with Asn225/Asn239 and Glu267/Glu281, the 3β-hydroxyl group of compound **6** forms more frequent hydrogen bonds with Asn225/Asn239, Arg305/Arg319 and Phe315/Phe329. The HBO values for these interactions are larger in the LXRβ complexes (Fig. 3e,f). Moreover, while the accessibility of water molecules to the 3α-hydroxyl of compound **5** is similar for both receptor isoforms, the solvation of the 3β-hydroxyl group of compound **6** is larger in the LXRα/**6** complex (Table 1). On the other hand, the oxygen atoms of the 2β,19-epoxy bridge of compounds **5** and **6** interact with Arg305/Arg319 in both LXRs. The superposition of representative snapshots of the LXRα/**6** and LXRβ/**6** complexes shows small variations in the conformation of polar residues interacting with the ligand (Fig. 4c), consistent with the similar activity profile of this compound with both isoforms.

3. Discussion

Taking the partial agonist DMHCA (**1**) as starting point, structural changes that bend the A ring towards the α face of the steroid nucleus as in **2** and **4** resulted in pure agonists, selective for the LXRα isoform. On the other hand, bending the A ring towards the β face as in **5** and **6** gave strong antagonists for both isoforms, with **6** being completely devoid of any agonistic activity. Despite the similarity of the ligand binding pockets of both isoforms, MD simulations show differences between LXRα- and LXRβ-ligand complexes, in the hydrogen bonding networks that involve the C-3 hydroxyl that correlate with differential activity on each isoform. In compounds **2** and **4** that exhibit selectivity towards the LXRα, the 3α-hydroxyl moves away from Leu316/330 and binds strongly to Ser264/276 increasing the H-bonding interaction with Glu281 in the LXRβ. The oxygen bridge in **4** adds a further interaction with Phe315/329, stronger for the LXRβ. In compounds **5** and **6**, the hydrogen bonding networks with LXRα and LXRβ are similar, which correlates with the similar activity profile observed for both isoforms. The oxygen bridge adds a specific interaction with Arg305/319 that is reinforced by the 3β-hydroxyl in the case of compound **6**.

Interestingly, although all compounds bind to the LXRs restricting the His421 (LXRα) or His435 (LXRβ) to give the so called "agonist conformation" of helix-12, changes in the A/B region of the steroid nucleus were able to switch from agonistic to antagonistic activity.

4. Conclusion

Although most ligands designed to regulate LXR activity are non-steroidal, the synthetic steroid DMHCA has emerged in recent years as very promising candidate, due to its ability to dissociate the beneficial from the undesirable effects. We showed here that certain structural modifications at the steroidal nucleus of DMHCA considerably alter the LXR response, in some cases selectively. The precise understanding of the molecular basis that governs this selectivity would be very valuable for the development of drugs with improved activity profile. Although further studies are still needed to fully assess whether these analogues conserve the dissociative properties of DMHCA, we consider that they may constitute

a new scaffold to achieve a propitious LXR modulation. Moreover, since these new compounds also present marked differences among their agonist/antagonist profile, they arise as useful tools for gaining further insight on LXR-mediated signaling networks.

5. Experimental

5.1. Chemistry

5.1.1. General

Mps were taken on a Fisher-Johns apparatus and are uncorrected. NMR spectra were recorded on an Avance II 500 NMR spectrometer (^{1}H at 500.13 MHz, ^{13}C at 125.77 MHz). Chemical shifts are given in ppm downfield from TMS as internal standard, J values are given in Hz. Multiplicity determinations and 2D spectra (COSY, NOESY, HSQC and HMBC) were obtained using standard Bruker software. Exact mass spectra were obtained using a Bruker micrOTOF-Q II mass spectrometer, equipped with an ESI source operating in positive mode. Flash chromatography was carried out on silica gel 60, 0.0040–0.0063 mm, Merck 9385. Medium Pressure Liquid Chromatography (MPLC) was carried out on a Buchi Sepacore purification system equipped with two pumps of 10 bar maximum pressure. Thin layer chromatography (tlc) analysis was performed on silica gel 60 F254 (0.2 mm thick). The homogeneity of all compounds was confirmed by tlc and ^{1}H NMR. Solvents were evaporated at reduced pressure and ca. 40–50 °C.

5.1.2. N,N-Dimethyl-3β-hydroxy-5-cholenamide (**1**)

General procedure: To a solution of 3β-hydroxy-5-cholenic acid methyl ester (50 mg, 0.13 mmol) in dry DMF (0.3 mL), dimethylamine hydrochloride (16 mg, 0.2 mmol), triethylamine (56 μL, 0.4 mmol) and a solution of (benzotriazol-1-yloxy) tris(dimethylamino)phosphonium hexafluorophosphate (89 mg, 0.2 mmol) in dry dichloromethane (0.3 mL) were successively added at 0 °C under an argon atmosphere. The reaction mixture was stirred at 0 °C for 30 min and then at 25 °C for 2 h. Water (5 mL) was added and the mixture was extracted with dichloromethane. The extract was washed with 1 N HCl and water, dried over anhydrous sodium sulfate and the solvent evaporated. The residue was purified by MPLC (flow rate: 20 mL/min, hexane-ethyl acetate 60:40 → hexane-ethyl acetate 30:70) to give (40 mg, 75%) identical (NMR) to that reported.[21]

5.1.3. N,N-Dimethyl-3α-hydroxy-5βH-cholanamide (**2**)

Amide **2** (51.0 mg, 95%) was obtained from lithocholic acid (50 mg, 0.133 mmol) (see general procedure); m.p. 168–170 °C; ^{1}H NMR (500 MHz, $CDCl_3$): δ 3.61 (1H, m, H-3), 3.00 (3H, s, CON$(CH_3)_2$), 2.93 (3H, s, CON$(CH_3)_2$), 2.34 (1H, m, H-23a), 2.19 (1H, m, H-23b), 1.95 (1H, m, H-12β), 1.86 (1H, m, H-16α), 1.84 (1H, m, H-6β), 1.78 (2H, m, H-22a and H-1β), 1.75 (1H, m, H-4α), 1.65 (1H, m, H-2α), 1.56 (1H, m, H-15α), 1.50 (1H, m, H-4β), 1.43 (1H, m, H-20), 1.40 (1H, m, H-7β), 1.38 (3H, m, H-8, H-9 and H-11α), 1.37 (1H, m, H-5), 1.33 (1H, m, H-2β), 1.32 (1H, m, H-22b), 1.28 (1H, m, H-16β), 1.25 (1H, m, H-6α), 1.23 (1H, m, H-11β), 1.14 (1H, m, H-12α), 1.10 (1H, m, H-17), 1.05 (1H, m, H-7α), 1.04 (2H, m, H-15β and H-14), 0.95 (1H, m, H-1α), 0.92 (3H, d, J = 6.5 Hz, H-21), 0.91 (3H, s, H-19), 0.64 (3H, s, H-18), ^{13}C NMR (125 MHz, $CDCl_3$): δ 173.7 (C-24), 71.9 (C-3), 56.5 (C-14), 56.1 (C-17), 42.7 (C-13), 42.1 (C-5), 40.4 (C-9), 40.2 (C-12), 36.5 (C-4), 35.8 (C-8), 35.6 (C-20), 35.3 (C-1), 34.6 (C-10), 31.2 (C-22), 30.5 (C-2), 30.3 (C-23), 28.2 (C-16), 27.2 (C-6), 26.4 (C-7), 24.2 (C-15), 23.4 (C-19), 20.8 (C-11), 18.5 (C-21), 12.5 (C-18); ESI-HRMS *m*/*z*: calcd for $C_{26}H_{45}NNaO_2$ $[M+Na]^+$ 426.3343, found 426.3336.

5.1.4. N,N-Dimethyl-3α,6α-dihydroxy-5βH-cholanamide (**3**)

Amide **3** (29.0 mg, 92%) was obtained from hyodeoxycholic acid (30.0 mg, 0.075 mmol) (see general procedure); m.p. 188–190 °C; ^{1}H NMR (500 MHz, $CDCl_3$): δ 4.05 (1H, dt, J = 12.3 and 4.7 Hz), 3.62 (1H, m, H-3), 3.01 (3H, s, CON$(CH_3)_2$), 2.94 (3H, s, CON$(CH_3)_2$), 2.37 (1H, m, H-23a), 2.22 (1H, m, H-23b), 1.98 (1H, m, H-12β), 1.92 (1H, m, H-4α), 1.90 (1H, m, H-16α), 1.80 (1H, m, H-1β), 1.79 (1H, m, H-22a), 1.70 (1H, m, H-2α), 1.64 (1H, m, H-7β), 1.68 (1H, m, H-5), 1.60 (1H, m, H-15α), 1.46 (1H, m, H-20), 1.44 (1H, m, H-8), 1.42 (2H, m, H-4β and H-11β), 1.38 (1H, m, H-9), 1.34 (2H, m, H-2β) and H-22b), 1.32 (1H, m, H-16β), 1.18 (1H, m, H-11β), 1.17 (1H, m, H-12α), 1.15 (2H, m, H-17 and H-7α), 1.13 (1H, m, H-14), 1.09 (1H, m, H-15β), 1.06 (1H, m, H-1α), 0.93 (3H, d, J = 6.6 Hz, H-21), 0.90 (3H, s, H-19), 0.64 (3H, s, H-18), ^{13}C NMR (125 MHz, $CDCl_3$): δ 173.7 (C-24), 71.5 (C-3), 68.0 (C-6), 56.1 (C-14), 56.0 (C-17), 48.4 (C-5), 42.8 (C-13), 39.9 (C-12), 39.8 (C-9), 37.3 (C-10), 35.9 (C-1), 35.6 (C-20), 35.0 (C-7), 34.8 (C-8), 31.1 (C-22), 30.3 (C-23), 30.2 (C-2), 29.3 (C-4), 28.1 (C-16), 24.2 (C-15), 23.5 (C-19), 20.7 (C-11), 18.4 (C-21), 12.0 (C-18); ESI-HRMS *m*/*z*: calcd for $C_{26}H_{46}NNaO_3$ $[M+Na]^+$ 442.3292, found 442.3285.

5.1.5. 3β-Acetoxy-5α-bromo-6β,19-epoxycholanic acid methyl ester (**8**)

3β-Hydroxy-5-cholenic acid methyl ester (3.70 g) was acetylated with acetic anhydride (37.0 mL) and pyridine (75.0 mL) to give the corresponding 3β-acetate **7**. To a stirred solution of this compound in ether (50.0 mL) and THF (19.0 mL), cooled to 10 °C was added 7.5% aqueous perchloric acid (6.0 mL) followed by *N*-bromoacetamide (2.00 g) in 8 portions during a 25 min period at 10–15 °C, protected from light. After 30 min at room temperature, 1% aqueous sodium thiosulphate was added, and the mixture was poured into dichloromethane/methanol (10:1 v/v). Extractive workup gave the 5α-bromo-6β-hydroxy derivative (5.0 g). The crude bromohydrin was dissolved in recently distilled dichloromethane (435 mL) and diacetoxyiodobenzene (4.1 g) and iodine (2.94 g) were added. The reaction mixture was vigorously stirred while irradiating with a 300 W tungsten lamp (5000 lm) for 30 min at 25 °C. After filtration, the solution was diluted with dichloromethane, washed with aqueous sodium thiosulfate, and the solvent evaporated. Purification of the residue by flash chromatography (hexane-ethyl acetate 80:20) gave the bromoether **8** (amorphous solid, 3.25 g, 64% from 3β-hydroxy-5-cholenic acid methyl ester); ^{1}H NMR (500 MHz, $CDCl_3$): δ 5.19 (1H, m, H-3), 4.05 (1H, d, J = 4.7 Hz, H-6), 3.98 (1H, d, J = 8.4 Hz, H-19a), 3.73 (1H, d, J = 8.3 Hz, H-19b), 3.66 (3H, s, OCH_3), 2.34 (1H, m, H-23a), 2.30 (1H, m, H-4α), 2.25 (1H, m, H-4β), 2.21 (1H, m, H-23b), 2.03 (3H, s, CH_3COO), 1.99 (2H, m, H-7β and H-2β), 1.97 (1H, m, H-12β), 1.88 (1H, m, H-15α), 1.79 (1H, m, H-22a), 1.69 (1H, m, H-7α), 1.66 (1H, m, H-9), 1.64 (1H, m, H-1α), 1.61 (1H, m, H-8), 1.52 (1H, m, H-16α and H-1α), 1.51 (1H, m, H-2α); 1.41 (1H, m, H-20), 1.39 (1H, m, H-11α), 1.32 (1H, m, H-22b), 1.28 (1H, m, H-15β), 1.23 (2H, m, H-12α and 1H, m, H-14), 1.15 (1H, m, H-11β), 1.13 (1H, m, H-17), 0.90 (3H, d, J = 6.5 Hz, H-21), 1.02 (1H, m, H-16β), 0.69 (3H, s, H-18); ^{13}C NMR (125 MHz, $CDCl_3$): δ 174.7 (C-24), 170.3 (3-CH_3**C**OO), 74.5 (C-5), 82.3 (C-6), 70.0 (C-3), 67.5 (C-19), 55.7 (C-17), 54.3 (C-14), 51.5 (OCH_3), 48.6 (C-9), 43.2 (C-13), 45.8 (C-10), 39.7 (C-12), 41.3 (C-4), 35.3 (C-20), 23.2 (C-1), 33.3 (C-8), 31.03 (C-23), 32.8 (C-7), 30.95 (C-22), 27.9 (C-2), 28.1 (C-16), 23.4 (C-15), 21.6 (C-11), 21.3 (3-**C**H_3COO), 18.2 (C-21), 12.4 (C-18); ESI-HRMS *m*/*z*: calcd for $C_{27}H_{41}BrNaO_5$ [M+Na]+ 547.2030, found 547.2033.

5.1.6. 3-Oxo-6β,19-epoxy-4-cholenic acid methyl ester (**9**)

To a solution of compound **8** (475 mg, 0.90 mmol) in THF (12.7 mL), K_2CO_3 (128 mg) in methanol (25.5 mL) was added and the mixture was stirred 1 h at 25 °C. Water was added and the reaction

mixture was neutralized with 1 N HCl (3.2 mL), concentrated to half of its volume and extracted with ethyl acetate. The organic layer was washed with water, dried with sodium sulfate and the solvent evaporated under vacuum. A suspension of pyridinium chlorochromate (302 mg, 1.39 mmol), barium carbonate (279 mg, 0.442 mmol) and 3 Å molecular sieves (441 mg) in anhydrous dichloromethane (34.8 mL) was stirred for 5 min under an Ar atmosphere at 25 °C. A solution of the residue obtained above in anhydrous dichloromethane (23.2 mL) was added and the stirring continued at 25 °C for 90 min. The reaction was diluted with ether, percolated through Celite eluting with ethyl acetate and the solvent was evaporated. The resulting solid was purified by flash chromatography (hexane-ethyl acetate 90:10 → 70:30) to give compound **9** (amorphous solid, 245 mg 0.61 mmol, 68% from **8**). ^{1}H NMR (500 MHz, $CDCl_3$): δ 5.81 (1H, s, H-4), 4.69 (1H, d, J = 5.2 Hz, H-6), 4.21 (1H, d, J = 8.1 Hz, H-19a), 3.66 (3H, s, OCH_3), 3.50 (1H, d, J = 8.1 Hz, H-19b), 2.36 (2H, m, H-2), 2.35 (1H, m, H-23a), 2.23 (1H, m, H-23b), 2.21 (1H, m, H-1α), 2.07 (1H, m, H-7β), 2.05 (1H, m, H-12β), 1.88 (1H, m, H-16α), 1.84 (1H, m, H-8), 1.81 (1H, m, H-1β), 1.80 (1H, m, H-22a), 1.58 (2H, m, H-11α and H-9), 1.52 (1H, m, H-15α), 1.45 (1H, m, H-11β), 1.43 (1H, m, H-20), 1.32 (1H, m, H-22b), 1.31 (1H, m, H-16β), 1.25 (1H, m, H-7α), 1.24 (1H, m, H-12α), 1.15 (2H, m, H-15β and H-14), 1.12 (1H, m, H-17), 0.92 (3H, d, J = 6.5 Hz, H-21), 0.75 (3H, s, H-18); ^{13}C NMR (125 MHz, $CDCl_3$): δ 199.0 (C-3), 174.7 (C-24), 172.2 (C-5), 114.8 (C-4), 77.3 (C-6), 75.6 (C-19), 55.6 (C-17), 54.7 (C-14), 51.5 (OCH_3), 50.2 (C-9), 46.0 (C-10), 43.5 (C-13), 41.2 (C-7), 39.4 (C-12), 35.3 (C-20), 33.7 (C-8), 33.3 (C-2), 31.0 (C-23), 30.9 (C-22), 28.1 (C-16), 26.5 (C-1), 24.1 (C-11), 23.7 (C-15), 18.2 (C-21), 12.3 (C-18); ESI-HRMS m/z: calcd for $C_{25}H_{36}NaO_4$ $[M+Na]^+$ 423.2506, found 423.2510.

*5.1.7. 3α-Hydroxy-6β,19-epoxy-4-cholenic acid methyl ester (**10**)*

Sodium borohydride (17.4 mg, 0.46 mmol) was added to a solution of compound **9** (90.0 mg, 0.23 mmol) in dichloromethane (2.0 mL) and methanol (2.0 mL) at 0 °C. The reaction mixture was stirred for 40 min at 25 °C, acidified (pH 6) with 1 N HCl and concentrated to a third of its volume. Water was added to the residue and then extracted with dichloromethane. The resulting solid was purified by flash chromatography (hexane-ethyl acetate 90:10 → 70:30) to give compound **10** (amorphous solid, 76.0 mg, 84%). ^{1}H NMR (500 MHz, $CDCl_3$): δ 5.48 (1H, d, J = 2.4 Hz, H-4), 4.45 (1H, d, J = 4.9 Hz, H-6), 4.07 (1H, d, J = 7.7 Hz, H-19a), 3.66 (3H, s, OCH_3), 3.32 (1H, d, J = 7.7 Hz, H-19b), 2.34 (1H, m, H-23a), 2.23 (1H, m, H-23b), 2.00 (1H, m, H-12β), 1.98 (1H, m, H-1α), 1.93 (1H, m, H-2β), 1.89 (1H, m, H-7β), 1.86 (1H, m, H-16α), 1.79 (1H, m, H-22a), 1.78 (1H, m, H-8), 1.54 (1H, m, H-11α), 1.52 (1H, m, H-2α), 1.50 (1H, m, H-15α), 1.46 (1H, m, H-9), 1.42 (1H, m, H-20), 1.32 (2H, m, H-1β and H-22b), 1.29 (1H, m, H-16β), 1.27 (1H, m, H-11β), 1.18 (2H, m, H-7α and H-12α), 1.14 (1H, m, H-14), 1.12 (1H, m, H-15β), 1.10 (1H, m, H-17), 0.93 (3H, d, J = 6.5 Hz, H-21), 0.74 (3H, s, H-18); ^{13}C NMR (125 MHz, $CDCl_3$): δ 174.7 (C-24), 149.6 (C-5), 115.5 (C-4), 77.1 (C-6), 75.3 (C-19), 67.6 (C-3), 55.7 (C-17), 55.0 (C-14), 51.5 (OCH_3), 50.2 (C-9), 44.3 (C-10), 43.3 (C-13), 39.7 (C-12), 39.6 (C-7), 35.3 (C-20), 34.3 (C-8), 31.05 (C-23), 30.95 (C-22), 29.0 (C-2), 28.1 (C-16), 25.1 (C-1), 23.6 (C-15), 22.9 (C-11), 18.2 (C-21), 12.3 (C-18); ESI-HRMS m/z: calcd for $C_{25}H_{38}NaO_4$ $[M+Na]+$ 425.26623, found 425.26616.

*5.1.8. 3α-Hydroxy-6β,19-epoxy-4-cholenic acid (**11**)*

To a solution of compound **10** (20 mg, 0.05 mmol) in a mixture of THF-MeOH 3:1 (2.2 mL), aqueous 5% lithium hydroxide was added (0.24 mL). After stirring at 25 °C for 2 h, water was added (3.5 mL), the mixture was acidified to pH 3 with 1 N HCl, concentrated to a third of its volume and extracted with ethyl acetate. The organic layer was washed with water, dried with sodium sulfate and the solvent evaporated. The resulting solid was purified by MPLC (flow rate: 20 mL/min, (hexane-ethyl acetate 70:30 → 50:50) to give acid **11** (amorphous solid, 13.0 mg, 67%). ^{1}H NMR (500 MHz, $CDCl_3$): δ 5.46 (1H, d, J = 2.4 Hz, H-4), 4.44 (1H, d, J = 4.8 Hz, H-6), 4.38 (1H, m, H-3), 4.06 (1H, d, J = 7.7 Hz, H-19a), 3.30 (1H, d, J = 7.7 Hz, H-19b), 2.39 (1H, m, H-23a), 2.26 (1H, m, H-23b), 2.00 (1H, m, H-12β), 1.97 (1H, m, H-1α), 1.94 (1H, m, H-2β), 1.89 (1H, m, H-7β), 1.86 (1H, m, H-16α), 1.81 (1H, m, H-22a), 1.78 (1H, m, H-8), 1.55 (1H, m, H-11α), 1.52 (1H, m, H-2α), 1.50 (1H, m, H-15α), 1.46 (1H, m, H-9), 1.45 (1H, m, H-20), 1.33 (1H, m, H-1β), 1.32 (1H, m, H-22b), 1.29 (1H, m, H-16β), 1.28 (1H, m, H-11β), 1.18 (2H, m, H-7α and H-12α), 1.14 (1H, m, H-14), 1.13 (1H, m, H-15β), 1.10 (1H, m, H-17), 0.93 (3H, d, J = 6.6 Hz, H-21), 0.73 (3H, s, H-18); ^{13}C NMR (125 MHz, $CDCl_3$): δ 178.8 (C-24), 149.6 (C-5), 115.4 (C-4), 77.1 (C-6), 75.3 (C-19), 67.6 (C-3), 55.7 (C-17), 55.0 (C-14), 50.2 (C-9), 44.3 (C-10), 43.4 (C-13), 39.7 (C-12), 39.6 (C-7), 35.3 (C-20), 34.3 (C-8), 30.8 (C-23), 30.7 (C-22), 28.9 (C-2), 28.2 (C-16), 25.1 (C-1), 23.7 (C-15), 22.9 (C-11), 18.2 (C-21), 12.3 (C-18); ESI-HRMS m/z: calcd for $C_{24}H_{36}NaO_4$ $[M+Na]+$ 411.25058, found 411.25028.

*5.1.9. N,N-Dimethyl-3α-hydroxy-6β,19-epoxy-4-cholenamide (**4**)*

The steroid acid **11** (25 mg, 0.064 mmol) was treated with a solution of (benzotriazol-1-yloxy)-tris(dimethylamino)phosphonium hexafluorophosphate in dry dichloromethane as previously described (General procedure) to give amide **4** after purification by MPLC (flow rate: 20 mL/min, hexane-ethyl acetate 50:50 → 0:100) (24.2 mg, 91%); m.p. 192–193 °C; ^{1}H NMR (500 MHz, $CDCl_3$): δ 5.47 (1H, d, J = 2.4 Hz, H-4), 4.45 (1H, d, J = 4.8 Hz, H-6), 4.05 (1H, d, J = 7.7 Hz, H-19a), 3.31 (1H, d, J = 7.7 Hz, H-19b), 3.02 (3H, s, $CON(CH_3)_2$), 2.95 (3H, s, $CON(CH_3)_2$), 2.35 (1H, m, H-23a), 2.21 (1H, m, H-23b), 2.01 (1H, m, H-12β), 1.98 (1H, m, H-1α), 1.93 (1H, m, H-2β), 1.89 (2H, m, H-7β and H-16α), 1.79 (1H, m, H-22a), 1.78 (1H, m, H-8), 1.55 (1H, m, H-11α), 1.52 (1H, m, H-2α), 1.49 (1H, m, H-15α), 1.46 (2H, m, H-9 and H-20), 1.33 (2H, m, H-1β and H-22b), 1.31 (1H, m, H-16β), 1.28 (1H, m, H-11β), 1.18 (2H, m, H-7α and H-12α), 1.14 (1H, m, H-15β), 1.13 (1H, m, H-14), 1.12 (1H, m, H-17), 0.95 (3H, d, J = 6.6 Hz, H-21), 0.73 (3H, s, H-18); ^{13}C NMR (125 MHz, $CDCl_3$): δ 173.6 (C-24), 149.7 (C-5), 115.4 (C-4), 77.1 (C-6), 75.3 (C-19), 67.6 (C-3), 55.9 (C-17), 55.0 (C-14), 50.2 (C-9), 44.3 (C-10), 43.4 (C-13), 39.7 (C-12), 39.6 (C-7), 37.4 and 35.4 ($CON(CH_3)_2$), 35.6 (C-20), 34.3 (C-8), 30.4 (C-23), 31.2 (C-22), 29.0 (C-2), 28.2 (C-16), 25.1 (C-1), 23.7 (C-15), 22.9 (C-11), 18.4 (C-21), 12.3 (C-18); ESI-HRMS m/z: calcd for $C_{26}H_{41}NNaO_3$ $[M+Na]^+$ 438.2979, found 438.2981.

*5.1.10. 3β-Acetoxy-19-hydroxy-5-cholenic acid methyl ester (**12**)*

To a solution of **8** (2.70 g, 5.15 mmol) in 2-propanol (275 mL) at 80 °C, acetic acid (3.8 mL) and activated Zn (3.40 g) were added. The suspension was stirred for 3 h at 80 °C. The mixture was cooled and filtered, the 2-propanol was evaporated under vacuum and the resulting solution was extracted with dichloromethane. The organic layer was washed with water, dried with sodium sulfate and the solvent evaporated. The resulting solid was recrystallized from methanol to give compound **12** (1.77 g, 80% from **8**); m.p. 138–139 °C; ^{1}H NMR (500 MHz, $CDCl_3$): δ 5.77 (1H, m, H-6), 4.64 (1H, m, H-3), 3.83 (1H, d, J = 10.9 Hz, H-19a), 3.66 (3H, s, OCH_3), 3.62 (1H, bs, H-19b), 2.42 (1H, m, H-4α), 2.35 (1H, m, H-23a), 2.27 (1H, td, J = 13.4 and 1.8 Hz, H-4β), 2.23 (1H, m, H-23b), 2.02 (2H, m, H-12β and H-7β), 2.03 (3H, s, CH_3COO), 1.96 (1H, m, H-1β), 1.87 (2H, m, H-2α and H-16α), 1.81 (1H, m, H-8), 1.80 (1H, m, H-22a), 1.58 (2H, m, H-11), 1.57 (1H, m, H-15α), 1.54 (1H, m, H-7α), 1.52 (1H, m, H-2β), 1.43 (1H, m, H-20), 1.33 (1H, m, H-22b), 1.30 (1H, m, H-16β), 1.16 (1H, m, H-12α), 1.14 (1H, m, H-1α), 1.10 (1H, m, H-17), 1.09 (1H, m, H-15β), 0.92 (3H, d, J = 6.5 Hz, H-21), 0.92 (1H, m, H-9), 0.91 (1H, m, H-14), 0.73 (3H, s,

H-18), ^{13}C NMR (125 MHz, $CDCl_3$): δ 174.7 (C-24), 170.5 (3-CH_3**C**OO), 134.5 (C-5), 128.3 (C-6), 73.4 (C-3), 62.7 (C-19), 57.5 (C-14), 55.7 (C-17), 51.5 (OCH_3), 50.2 (C-9), 42.6 (C-13), 41.6 (C-10), 39.9 (C-12), 38.2 (C-4), 35.4 (C-20), 33.4 (C-8), 33.1 (C-1), 31.2 (C-7), 31.06 (C-23), 31.00 (C-22), 28.1 (C-2 and C-16), 24.0 (C-15), 21.7 (C-11), 21.4 (3-**C**H_3COO), 18.3 (C-21), 12.2 (C-18); ESI-HRMS *m*/*z*: calcd for $C_{27}H_{42}NaO_5$ $[M+Na]^+$ 469.2924, found 469.2919.

*5.1.11. 3β,19-Diacetoxy-5αH-cholanic acid methyl ester (**13**)*

Acetylation of **12** (2.41 g, 4.91 mmol) in dichloromethane (40 mL) with acetic anhydride (27 mL), pyridine (53.0 mL) and DMAP (1.0 mg) at 25 °C for 3 h, followed by purification by flash chromatography (hexane – ethyl acetate 95:5 → 90:10) gave the 19-acetoxy steroid. To a solution of the latter product (2.00 g, 4.47 mmol) in ethyl acetate (45.0 mL) and ethanol (45 mL), Pd/C 10% w/w (300 mg) was added and the resulting mixture was hydrogenated at 50 psi and 25 °C for 24 h. The reaction mixture was then filtered through a silica gel pad and the filter was washed with ethyl acetate. The filtrate was evaporated under reduced pressure to give compound **13** (amorphous solid, 1.96 mg, 98% from **12**).^{1}H NMR (500 MHz, $CDCl_3$): δ 4.72 (1H, m, H-3), 4.32 (1H, d, *J* = 12.1 Hz, H-19a), 4.23 (1H, d, *J* = 12.1 Hz, H-19b), 3.66 (3H, s, OCH_3), 2.33 (1H, ddd, *J* = 15.5, 10.4 and 5.2 Hz, H-23a), 2.22 (1H, m, H-23b), 2.21 (1H, m, H-1β), 2.07 (3H, s, 19-CH_3COO), 2.02 (3H, s, 3-CH_3COO), 1.94 (1H, m, H-12β), 1.85 (1H, m, H-16α), 1.84 (1H, m, H-2α), 1.78 (1H, m, H-22a), 1.71 (1H, m, H-4α), 1.70 (1H, m, H-7β), 1.57 (1H, m, H-15α), 1.56 (1H, m, H-11α), 1.46 (1H, m, H-4β), 1.45 (1H, m, H-8), 1.42 (1H, m, H-20), 1.40 (1H, m, H-2β), 1.36 (1H, m, H-11β), 1.33 (2H, m, H-5 and H-22b), 1.26 (2H, m, H-6 and H-16β), 1.08 (2H, m, H-17 and H-15β), 1.07 (1H, m, H-12α), 1.01 (1H, m, H-14), 0.93 (1H, m, H-1α), 0.92 (1H, m, H-7α), 0.90 (3H, d, *J* = 6.5 Hz, H-21), 0.74 (1H, m, H-9), 0.64 (3H, s, H-18), ^{13}C NMR (125 MHz, $CDCl_3$): δ 174.7 (C-24), 171.2 (19-CH_3-**C**OO), 170.7 (3-CH_3**C**OO), 73.0 (C-3), 62.7 (C-19), 56.6 (C-14), 55.8 (C-17), 54.1 (C-9), 51.5 (OCH_3), 44.7 (C-5), 42.6 (C-13), 40.2 (C-12), 37.9 (C-10), 35.8 (C-8), 35.4 (C-20), 34.2 (C-4), 31.8 (C-7), 31.6 (C-1), 31.04 (C-23), 30.96 (C-22), 28.1 (C-6), 28.0 (C-16), 27.5 (C-2), 24.1 (C-15), 22.2 (C-11), 21.4 (19-CH_3**C**OO), 21.2 (3-**C**H_3COO), 18.2 (C-21), 12.1 (C-18); ESI-HRMS *m*/*z*: calcd for $C_{29}H_{46}Na_6$ $[M+Na]^+$ 513.3187, found 513.3190.

*5.1.12. 3β-Hydroxy-19-acetoxy-5βH-cholanic acid methyl ester (**14**)*

Compound **13** (1.89 g, 4.23 mmol) in THF (60.0 mL), was treated with K_2CO_3 (600 mg) in methanol (120 mL) as previously described for **9**. The resulting solid was purified by flash chromatography (hexane-ethyl acetate 90:10 → 80:20) to give compound **14** (amorphous solid, 1.26 g, 74%); ^{1}H NMR (500 MHz, $CDCl_3$): δ 4.33 (1H, d, *J* = 12.1 Hz, H-19a), 4.20 (1H, d, *J* = 12.1 Hz, H-19b), 3.66 (3H, s, OCH_3), 3.65 (1H, m, H-3), 2.34 (1H, ddd, *J* = 15.5, 10.4 and 5.2 Hz, H-23a), 2.22 (1H, m, H-23b), 2.20 (1H, m, H-1β), 2.06 (3H, s, 19-CH_3COO), 1.94 (1H, m, H-12β), 1.85 (1H, m, H-16α), 1.84 (1H, m, H-2α), 1.78 (1H, m, H-22a), 1.71 (1H, m, H-7β), 1.68 (1H, m, H-4α), 1.59 (1H, m, H-11α), 1.57 (1H, m, H-15α), 1.47 (1H, m, H-8), 1.40 (1H, m, H-20), 1.38 (1H, m, H-4β), 1.34 (1H, m, H-11β), 1.32 (1H, m, H-22b), 1.31 (1H, m, H-2β), 1.28 (1H, m, H-16β), 1.27 (3H, m, H-5 and H-6), 1.08 (2H, m, H-17 and H-15β), 1.07 (1H, m, H-12α), 1.00 (1H, m, H-14), 0.90 (1H, m, H-7α), 0.90 (3H, d, *J* = 6.5 Hz, H-21), 0.89 (1H, m, H-1α), 0.72 (1H, m, H-9), 0.64 (3H, s, H-18); ^{13}C NMR (125 MHz, $CDCl_3$): δ 174.7 (C-24), 171.2 (19-CH_3**C**OO), 70.9 (C-3), 62.8 (C-19), 56.7 (C-14), 55.8 (C-17), 54.3 (C-9), 51.5 (OCH_3), 45.0 (C-5), 42.6 (C-13), 40.3 (C-12), 38.4 (C-4), 37.8 (C-10), 35.8 (C-8), 35.4 (C-20), 31.9 (C-7), 31.8 (C-1), 31.6 (C-2), 31.04 (C-23), 30.97 (C-22), 28.2 (C-6), 28.0 (C-16), 24.1 (C-15), 22.3 (C-11), 21.2 (3-**C**H_3COO), 18.2 (C-21), 12.1 (C-18); ESI-HRMS *m*/*z*: calcd for $C_{27}H_{44}NaO_5$ $[M+Na]^+$ 471.3081, found 471.3089.

*5.1.13. 19-Acetoxy-5βH-2-cholenic acid methyl ester (**15**)*

Trifluoromethanesulfonic anhydride (75.0 μL) was slowly added to a solution of compound **14** (100 mg, 0.22 mmol) in dichloromethane (1.0 mL) at −20 °C under a N_2 atmosphere. After completion of the addition the reaction was stirred for 30 min, then an aqueous solution of sodium acetate (72.0 mg in 0.1 mL) was added and the reaction was stirred at −20 °C for 5 min. The reaction mixture was allowed to warm to room temperature and extracted with dichloromethane and water. The organic layer was washed with water, dried with sodium sulfate and the solvent evaporated under vacuum. The resulting solid was purified by MPLC (flow rate: 20 mL/min, hexane → hexane-ethyl acetate 95:5) to give compound **15** (amorphous solid, 70 mg, 73%). ^{1}H NMR (500 MHz, $CDCl_3$): δ 5.62 (2H, m, H-2 and H-3), 4.31 (1H, d, *J* = 11.8 Hz, H-19a), 4.07 (1H, d, *J* = 11.8 Hz, H-19b), 3.66 (3H, s, OCH_3), 2.34 (1H, m, H-23a), 2.30 (1H, m, H-4β), 2.23 (1H, m, H-23b), 2.03 (3H, s, CH_3COO), 1.98 (1H, m, H-12β), 1.96 (1H, m, H-1β), 1.85 (1H, m, H-16α), 1.82 (1H, m, H-1α), 1.79 (1H, m, H-22a), 1.74 (1H, m, H-7β), 1.65 (1H, m, H-4α), 1.60 (1H, m, H-15α), 1.56 (1H, m, H-5), 1.55 (1H, m, H-11α), 1.51 (1H, m, H-8), 1.47 (1H, m, H-11β), 1.46 (1H, m, H-6α), 1.42 (1H, m, H-20), 1.35 (1H, m, H-6β), 1.32 (1H, m, H-22b), 1.28 (1H, m, H-16β), 1.10 (1H, m, H-17), 1.09 (1H, m, H-12α), 1.07 (1H, m, H-15β), 0.97 (1H, m, H-14), 0.93 (1H, m, H-7α), 0.91 (3H, d, *J* = 6.5 Hz, H-21), 0.83 (1H, m, H-9), 0.65 (3H, s, H-18); ^{13}C NMR (125 MHz, $CDCl_3$): δ 174.7 (C-24), 171.2 (19-CH_3**C**OO), 126.1–125.5 (C-2 and C-3), 63.5 (C-19), 56.9 (C-14), 55.8 (C-17), 54.0 (C-9), 51.5 (OCH_3), 42.5 (C-13), 41.5 (C-5), 40.2 (C-12), 37.4 (C-10), 36.1 (C-8), 35.4 (C-20), 34.7 (C-4), 31.7 (C-7), 31.04 (C-23), 30.98 (C-22), 30.4 (C-1), 28.6 (C-6), 28.0 (C-16), 24.1 (C-15), 21.7 (C-11), 21.3 (3-**C**H_3COO), 18.2 (C-21), 12.0 (C-18); ESI-HRMS *m*/*z*: calcd for $C_{27}H_{42}NaO_4$ $[M+Na]^+$ 453.2975, found 453.2965.

*5.1.14. 19-Acetoxy-2α,3α-epoxy-5αH-cholanic acid methyl ester (**16**)*

To a solution of **15** (113 mg, 0.262 mmol) in dichloromethane (15 mL) were added Na_2CO_3 (245 mg) in water (4.9 mL) and 3-chloroperoxybenzoic acid (245 mg, 1.42 mmol) in dichloromethane (9.0 mL), and the mixture was vigorously stirred at 0 °C for 1 h and then at 25 °C for 2 h. The mixture was diluted with dichloromethane (27 mL) and the aqueous layer was extracted with dichloromethane. The organic layer was washed with 5% aqueous Na_2SO_3, saturated aqueous $NaHCO_3$ and water, dried with sodium sulfate and the solvent evaporated. The resulting solid was purified by MPLC (flow rate: 20 mL/min, hexane → hexane-ethyl acetate 75:25) to give compound **16** (amorphous solid, 91.0 mg, 79%); ^{1}H NMR (500 MHz, $CDCl_3$): δ 4.18 (1H, d, *J* = 11.9 Hz, H-19a), 4.14 (1H, d, *J* = 11.8 Hz, H-19b), 3.66 (3H, s, OCH_3), 3.15 (1H, m, H-2), 3.12 (1H, m, H-3), 2.34 (1H, m, H-23a), 2.22 (1H, m, H-23b), 2.15 (1H, m, H-4β), 2.05 (3H, s, CH_3COO), 1.96 (1H, m, H-12β), 1.95 (1H, m, H-1β), 1.84 (2H, m, H-6α and H-16α), 1.78 (1H, m, H-22a), 1.69 (1H, m, H-7β), 1.61 (1H, m, H-1α), 1.58 (1H, m, H-15α), 1.50 (1H, m, H-11α), 1.47 (1H, m, H-8), 1.46 (1H, m, H-6α), 1.45 (1H, m, H-4α), 1.41 (1H, m, H-20), 1.40 (1H, m, H-11β), 1.37 (1H, m, H-16β), 1.31 (1H, m, H-22b), 1.28 (1H, m, H-6β), 1.26 (1H, m, H-5), 1.08 (1H, m, H-12α), 1.07 (1H, m, H-17), 1.03 (1H, m, H-15β), 0.90 (1H, m, H-14), 0.90 (3H, d, *J* = 6.5 Hz, H-21), 0.86 (1H, m, H-7α), 0.74 (1H, m, H-9), 0.63 (3H, s, H-18); ^{13}C NMR (125 MHz, $CDCl_3$): δ 174.7 (C-24), 170.9 (19-CH_3**C**OO), 63.8 (C-19), 56.7 (C-14), 55.7 (C-17), 53.6 (C-9), 52.7 (C-2), 51.4 (OCH_3), 51.3 (C-3), 42.4 (C-13), 39.9 (C-12), 36.4 (C-10), 36.2 (C-8), 36.0 (C-5), 35.3 (C-20), 34.0 (C-4), 31.5 (C-7), 30.99 (C-23), 30.92 (C-22), 29.5 (C-1), 28.2 (C-16), 28.0 (C-6), 24.1 (C-15), 21.22 (C-11), 21.18 (19-CH_3**C**OO), 18.2 (C-21), 12.0 (C-18); ESI-HRMS *m*/*z*: calcd for $C_{27}H_{42}NaO_5$ $[M+Na]^+$ 469.2925, found 469.2929.

*5.1.15. 3α-Hydroxy-2β,19-epoxy-5αH-cholanic acid methyl ester (**17**)*

To a solution of compound **16** (100 mg, 0.22 mmol) in methanol (2 mL), a solution of sodium methoxide (60 mg, 1.1 mmol) in methanol (5 mL) was added at 0 °C under a N_2 atmosphere and the reaction mixture was heated at 40 °C for 4 h. The mixture was diluted with water (5 mL), concentrated to a third of its volume by evaporation under reduced pressure and extracted with dichloromethane. The organic layer was washed with water, dried with sodium sulfate and the solvent evaporated. The resulting solid was purified by MPLC (flow rate: 20 mL/min, hexane → hexane-ethyl acetate 50:50) to give compound **17** (amorphous solid, 70 mg, 80%); ^{1}H NMR (500 MHz, $CDCl_3$): δ 4.14 (1H, dd, J = 6.1 and 4.9 Hz, H-2), 3.89 (1H, m, H-3), 3.75 (1H, d, J = 8.1 Hz, H-19a), 3.66 (1H, d, J = 8.1 Hz, H-19b), 3.66 (3H, s, OCH_3), 2.34 (1H, m H-23a), 2.21 (1H, m, H-23b), 2.00 (1H, m, H-12β), 1.96 (1H, m, H-1α), 1.85 (1H, m, H-16α), 1.78 (1H, m, H-22a), 1.70 (1H, m, H-1β), 1.67 (1H, m, H-5), 1.66 (1H, m, H-7β), 1.65 (1H, m, H-11b), 1.59 (1H, m, H-15α), 1.52 (2H, m, H-4), 1.49 (1H, m, H-6α), 1.41 (1H, m, H-20), 1.34 (1H, m, H-11α), 1.31 (1H, m, H-22b), 1.27 (1H, m, H-16β), 1.16 (1H, m, H-12α), 1.15 (2H, m, H-6β and H-9), 1.10 (1H, m, H-17) 1.02 (1H, m, H-15β), 0.98 (1H, m, H-14), 0.91 (3H, d, J = 6.6 Hz, H-21), 0.87 (1H, m, H-8 and H-7α), 0.62 (3H, s, H-18); ^{13}C NMR (125 MHz, $CDCl_3$): δ 174.7 (C-24), 77.6 (C-2), 68.7 (C-3), 66.4 (C-19), 56.5 (C-14), 55.8 (C-17), 51.5 (OCH_3), 46.9 (C-10), 46.2 (C-9), 42.3 (C-13), 39.8 (C-5), 39.6 (C-12), 38.5 (C-8), 35.5 (C-4), 35.5 (C-20), 34.8 (C-1), 31.3 (C-7), 31.04 (C-23), 30.96 (C-22), 30.0 (C-6), 28.1 (C-16), 24.1 (C-15), 20.9 (C-11), 18.3 (C-21), 11.8 (C-18); ESI-HRMS m/z: calcd for $C_{25}H_{40}NaO_4$ $[M+Na]^+$ 427.2819, found 427.2806.

*5.1.16. N,N-Dimethyl-3α-hydroxy-2β,19-epoxy-5βH-cholanamide (**5**)*

Compound **17** (20 mg, 0.05 mmol) in a mixture of THF-MeOH 3:1 (2.1 mL) was treated with aqueous 5% lithium hydroxide as previously described for **11**. The resulting acid was converted to the amide **5** following the general procedure described above. The crude material was crystallized from chloroform/*n*-hexane to give **5** (20 mg, 89% from **17**); m.p. 190–192 °C; ^{1}H NMR (500 MHz, $CDCl_3$): δ 4.14 (1H, dd, J = 6.1 and 4.9 Hz, H-2), 3.89 (1H, m, H-3), 3.75 (1H, d, J = 8.1 Hz, H-19a), 3.66 (1H, d, J = 8.1 Hz, H-19b), 3.00 (3H, s, 24-CON(CH_3)$_2$), 2.94 (3H, m, 24-CON(CH_3)$_2$), 2.35 (1H, m, H-23a), 2.20 (1H, m, H-23b), 2.01 (1H, m, H-12β), 1.96 (1H, m, H-1α), 1.88 (1H, m, H-16α), 1.78 (1H, m, H-22a), 1.72 (1H, m, H-1β), 1.68 (1H, m, H-5), 1.66 (1H, m, H-7β), 1.65 (1H, m, H-11β), 1.59 (1H, m, H-15α), 1.53 (2H, m, H-4), 1.50 (1H, m, H-6α), 1.44 (1H, m, H-20), 1.35 (1H, m, H-11α), 1.33 (1H, m, H-22b), 1.30 (1H, m, H-16β), 1.17 (1H, m, H-12α), 1.16 (2H, m, H-6β and H-9), 1.12 (1H, m, H-17), 1.01 (1H, m, H-15β), 0.98 (1H, m, H-14), 0.94 (3H, d, J = 6.6 Hz, H-21), 0.88 (2H, m, H-8 and H-7α), 0.62 (3H, s, H-18); ^{13}C NMR (125 MHz, $CDCl_3$): δ 173.7 (C-24), 77.6 (C-2), 68.7 (C-3), 66.5 (C-19), 56.6 (C-17), 56.0 (C-14), 46.9 (C-10), 46.2 (C-9), 42.3 (C-13), 39.8 (C-5), 39.6 (C-12), 38.5 (C-8), 37.3 (24-CON(CH_3)$_2$), 35.6 (C-20), 35.5 (C-4), 35.4 (24-CON(CH_3)$_2$), 34.8 (C-1), 31.3 (C-7), 31.2 (C-22), 30.4 (C-23), 30.0 (C-6), 28.1 (C-16), 24.1 (C-15), 20.9 (C-11), 18.5 (C-21), 11.9 (C-18); ESI-HRMS m/z: calcd for $C_{26}H_{44}NO_3$ $[M+H]^+$ 418.3316, found 418.3311.

*5.1.17. N,N-Dimethyl-3β-hydroxy-2β,19-epoxy-5αH-cholanamide (**6**)*

Compound **5** (13 mg, 0.031 mmol) in anhydrous dichloromethane (1.0 mL) was treated with a suspension of pyridinium chlorochromate (13 mg, 0.060 mmol), barium carbonate (12 mg, 0.019 mmol) and 3 Å molecular sieves (19 mg) in anhydrous dichloromethane (1.5 mL) as previously described for **9**. The resulting ketone was dissolved in anhydrous THF (0.5 mL) and a 1 M solution of lithium tri(*t*-butoxy)aluminum hydride in anhydrous THF (0.140 mL, 0.140 mmol) was added at 0 °C under an Ar atmosphere. The resulting solution was stirred for 2 h at 0 °C and then acidified to pH 2 with a aqueous $KHSO_4$. Extraction with dichloromethane followed by preparative tlc (toluene-ethyl acetate 40:60) gave compound **6** (5.8 mg, 45%) and compound **5** (2.9 mg, 22%). Compound **6**: m.p. 173–175 °C; ^{1}H NMR (500 MHz, $CDCl_3$): δ 4.12 (1H, d, J = 7.1 Hz, H-2), 3.74 (1H, d, J = 8.0 Hz, H-19b), 3.70 (1H, d, J = 8.3 Hz, H-19a), 3.51 (1H, m, H-3), 3.00 (3H, s, 24-CON(CH_3)$_2$), 2.94 (3H, m, 24-CON(CH_3)$_2$), 2.37 (1H, m, H-23a), 2.22 (1H, m, H-23b), 2.03 (1H, m, H-12β), 2.24 (1H, m, H-1α), 2.02 (1H, m, H-4α), 1.88 (1H, m, H-16α), 1.80 (1H, m, H-22a), 1.14 (1H, m, H-1β), 1.41 (1H, m, H-5), 1.58 (1H, m, H-7α), 1.65 (1H, m, H-11β), 1.60 (1H, m, H-15α), 1.13 (1H, m, H-4β), 1.70 (1H, m, H-6β), 1.46 (1H, m, H-20), 1.40 (1H, m, H-11α), 1.34 (1H, m, H-22b), 1.32 (1H, m, H-16β), 1.18 (1H, m, H-12α), 0.88 (1H, m, H-6α), 1.13 (1H, m, H-9), 1.14 (1H, m, H-17), 1.04 (1H, m, H-15β), 0.98 (1H, m, H-14), 0.93 (3H, d, J = 6.6 Hz, H-21), 0.89 (1H, m, H-8), 1.21 (1H, m, H-7β), 0.62 (3H, s, H-18); ^{13}C NMR (125 MHz, $CDCl_3$): δ 173.6 (C-24), 79.9 (C-2), 72.0 (C-3), 67.8 (C-19), 56.5 (C-14), 56.0 (C-17), 46.4 (C-10), 46.0 (C-9), 42.4 (C-13), 42.2 (C-5), 39.6 (C-12), 38.8 (C-1), 38.5 (C-8), 37.4 (C-4), 37.3 (24-CON(CH_3)$_2$), 35.6 (C-20), 35.4 (24-CON(CH_3)$_2$), 31.4 (C-7), 31.2 (C-22), 30.4 (C-23), 30.2 (C-6), 28.2 (C-16), 24.2 (C-15), 21.3 (C-11), 18.5 (C-21), 11.9 (C-18); ESI-HRMS m/z: calcd for $C_{26}H_{44}NO_3$ $[M+H]^+$ 418.3316, found 418.3315.

5.2. Biological activity

5.2.1. Cell culture and transient transfections

BHK21 cells were cultured at 37 °C under 5% CO_2 humidified atmosphere in high glucose DMEM supplemented with 10% fetal calf serum (FCS) containing penicillin (100 IU/mL), streptomycin (100 mg/mL) and glutamine (2 mM) in p100 plates. For transient transfections, 1×10^5 cells were plated in 24-wells plates and transfected with lipofectamine according to the manufacturer protocol (Lipofectamine 2000, Invitrogen). Analyses of human LXRβ or human LXRα activities were performed by transfecting 0.44 μg of the reporter construct pGL3/LRELuc, which consists of three copies of AGGTCAagccAGGTCA fused to nucleotides −56 to +109 of the human *c-fos* promoter in front of the firefly luciferase gene in the plasmid basic pGL3; 0.36 μg of the respective CMX-hLXRα or pSG5-hLXRβ expression vectors (kindly provided by Dr. Shutsung Liao, University of Chicago), 0.15 μg of human pSG5/hRXRα and 0.40 μg of pRSV-LacZ (Clontech Inc., Palo Alto, CA) as control of transfection. After transfection, the medium was replaced by serum-free medium containing antibiotics. Cells were then incubated during 18 h with GW3965 (Sigma), DMHCA (**1**) and compounds **2**–**6** at the indicated concentrations. Ligands were applied from 1000-fold stock solutions in dimethylsulfoxide (DMSO). Incubations were stopped by aspirating the medium and washing the cells twice with phosphate buffered saline solution (PBS). Cells were then harvested in lysis buffer and luciferase activity was measured according to the manufacturer protocol (Promega Inc.). Galactosidase activity was measured as previously described.[22] Statistical analyses were performed with GraphPad Prism 5 (GraphPad Software Inc.) and followed by Dunnett's test. Differences were regarded as significant at $p < 0.05$.

5.3. Computational methods

5.3.1. Initial structures of LXR/ligand complexes

The starting coordinates of the human LXRβ ligand binding domain was taken from the crystal structure of the LXRα/24S,25-epoxycholesterol complex (pdb: 1p8d, chain A). The four missing residues of the H1-H3 loop (255–258) were modeled with the Modeller program.[23] In order to build the LXRβ/ligand complexes, the HF/6-31G** optimized structures of the steroids were

introduced by superimposing the skeleton carbon atoms of C and D rings with the corresponding atoms of 24S,25-epoxycholesterol. Since no crystal structures of LXRα/steroid complex had been resolved yet, the starting coordinates of the human LXRα ligand binding domain was taken from the crystal structure of the complex with a non steroidal ligand (pdb: 5avi, chain A). Again, the missing residues of the H1 helix and the H1-H3 loop (223 to 233 and 240 to 243) were added with the Modeller program, but now using the LXRβ backbone structure as template. The LXRα/ligand complexes were then constructed by superimposing the protein backbone atoms of the LXRβ/ligand complexes with the protein backbone atoms of the LXRα model, and extracting the ligand coordinates. The corresponding force field parameters of the ligand, RESP (restraint electrostatic potential) atomic partial charges were computed using the HF/6-31G** method in the quantum chemistry program Gaussian 09[24] for the corresponding optimized structures.

5.3.2. Molecular dynamics

Molecular dynamics (MD) were performed with the AMBER 14 software package.[25] Ligand parameters were assigned according to the general AMBER force field (GAFF) and the corresponding RESP charges using the Antechamber. The FF14SB force field parameters were used for all receptor residues. Complexes were immersed in an octahedral box of TIP3P water molecules using the Tleap module, giving final systems of around 35,000 atoms. Systems were initially optimized and then gradually heated to a final temperature of 300 K. Starting from these equilibrated structures, MD production runs of 50 ns were performed. The production runs were performed at 300 K in a NPT ensemble using periodic boundary conditions and the particle mesh Ewald method (grid spacing of 1 Å) for treating long-range electrostatic interactions with a uniform neutralizing plasma. Temperature regulation was done using a by Langevin thermostat with a collision frequency of 2 ps^{-1}. The SHAKE algorithm was used to keep bonds involving H atoms at their equilibrium length, allowing the use of a 2 fs time step for the integration of Newton's equations.

5.3.3. Analysis of results

Trajectories were analyzed with the CPPTRAJ module.[26] Hydrogen bond occupancy (HBO) for each interaction was calculated with the hbond command using the default parameters for the distance cutoff (acceptor to donor heavy atom less than 3.0 Å) and for the angle cutoff (135°). Representative snapshots of each simulated system were obtained with the cluster command using the Density-Based Spatial Clustering of Applications with Noise (DBSCAN) algorithm and the RMSD of ligand and LBP atoms as distance metric. Trajectories and representative snapshots were visualized with VMD.[27]

Acknowledgements

This work was supported by Agencia Nacional de Promoción Científica y Tecnológica (PICT 2014-0626), CONICET-Argentina (PIP 112-201101-00702) and Universidad de Buenos Aires (Grant 20020130100367).

A. Supplementary data

Supplementary data associated with this article can be found, in the online version, at https://doi.org/10.1016/j.bmc.2018.01.025.

References

1. Gabbi C, Warner M, Gustafsson JA. Action mechanisms of Liver X Receptors. *Biochem Biophys Res Commun*. 2014;446:647–650.
2. Jakobsson T, Treuter E, Gustafsson JA, Steffensen KR. Liver X receptor biology and pharmacology: new pathways, challenges and opportunities. *Trends Pharmacol Sci*. 2012;33:394–404.
3. Tice CM, Noto PB, Fan KY, Zhuang L, Lala DS, Singh SB. The medicinal chemistry of liver X receptor (LXR) modulators. *J Med Chem*. 2014;57:7182–7205.
4. Hong C, Tontonoz P. Liver X receptors in lipid metabolism: opportunities for drug discovery. *Nat Rev Drug Discov*. 2014;13:433–444.
5. Im SS, Osborne TF. Liver x receptors in atherosclerosis and inflammation. *Circ Res*. 2011;108:996–1001.
6. Viennois E, Mouzat K, Dufour J, Morel L, Lobaccaro JM, Baron S. Selective liver X receptor modulators (SLiMs): what use in human health? *Mol Cell Endocrinol*. 2012;351:129–141.
7. Repa JJ, Liang G, Ou J, et al. Regulation of mouse sterol regulatory element-binding protein-1c gene (SREBP-1c) by oxysterol receptors, LXRalpha and LXRbeta. *Genes Dev*. 2000;14:2819–2830.
8. Phelan CA, Weaver JM, Steger DJ, et al. Selective partial agonism of liver X receptor alpha is related to differential corepressor recruitment. *Mol Endocrinol*. 2008;22:2241–2249.
9. Torocsik D, Szanto A, Nagy L. Oxysterol signaling links cholesterol metabolism and inflammation via the liver X receptor in macrophages. *Mol Aspects Med*. 2009;30:134–152.
10. Zhao C, Dahlman-Wright K. Liver X receptor in cholesterol metabolism. *J Endocrinol*. 2010;204:233–240.
11. Song C, Liao S. Cholestenoic acid is a naturally occurring ligand for liver X receptor alpha. *Endocrinology*. 2000;141:4180–4184.
12. Quinet EM, Savio DA, Halpern AR, Chen L, Miller CP, Nambi P. Gene-selective modulation by a synthetic oxysterol ligand of the liver X receptor. *J Lipid Res*. 2004;45:1929–1942.
13. Kratzer A, Buchebner M, Pfeifer T, et al. Synthetic LXR agonist attenuates plaque formation in apoE-/- mice without inducing liver steatosis and hypertriglyceridemia. *J Lipid Res*. 2009;50:312–326.
14. Yu S, Li S, Henke A, et al. Dissociated sterol-based liver X receptor agonists as therapeutics for chronic inflammatory diseases. *FASEB J*. 2016;30:2570–2579.
15. Alvarez LD, Dansey MV, Grinman DY, et al. Destabilization of the torsioned conformation of a ligand side chain inverts the LXRbeta activity. *Biochim Biophys Acta Mol Cell Biol Lip*. 2015;1851:1577–1586.
16. Viktorsson EO, Gabrielsen M, Kumarachandran N, et al. Regulation of liver X receptor target genes by 22-functionalized oxysterols. Synthesis, in silico and in vitro evaluations. *Steroids*. 2017;118:119–127.
17. Peng D, Hiipakka RA, Dai Q, et al. Antiatherosclerotic effects of a novel synthetic tissue-selective steroidal liver X receptor agonist in low-density lipoprotein receptor-deficient mice. *J Pharmacol Exp Ther*. 2008;327:332–342.
18. Fu J, Cheng K, Zhang ZM, Fang RQ, Zhu HL. Synthesis, structure and structure-activity relationship analysis of caffeic acid amides as potential antimicrobials. *Eur J Med Chem*. 2010;45:2638–2643.
19. Kumar Raju Ranjith, Haveli SD, Kagan Henri B. A mild one-pot method for conversion of various steroidal secondary alcohols into the corresponding olefins. *Synlett*. 2011;12:1709–1712.
20. Eduardo SL, Ghini AA, Burton G. Oxido-bridged neurosteroid analogues. Synthesis of 2,19-oxido-allopregnanolone. *ARKIVOC*. 2003;468–476.
21. Karaki F, Ohgane K, Dodo K, Hashimoto Y. Structure-activity relationship studies of Niemann-Pick type C1-like 1 (NPC1L1) ligands identified by screening assay monitoring pharmacological chaperone effect. *Bioorg Med Chem*. 2013;21:5297–5309.
22. Truss M, Bartsch J, Schelbert A, Hache RJ, Beato M. Hormone induces binding of receptors and transcription factors to a rearranged nucleosome on the MMTV promoter in vivo. *EMBO J*. 1995;14:1737–1751.
23. Sali A, Blundell TL. Comparative protein modelling by satisfaction of spatial restraints. *J Mol Biol*. 1993;234:779–815.
24. Frisch MJ, Schlegel HB, Scuseria GE, et al. *Gaussian 09*. Wallingford, CT, USA: Gaussian Inc; 2009.
25. Case DA, Betz RM, Cerutti DS, et al. *AMBER 2015*. San Francisco: University of California; 2015.
26. Roe DR, Cheatham 3rd TE. PTRAJ and CPPTRAJ: software for processing and analysis of molecular dynamics trajectory data. *J Chem Theory Comput*. 2013;9:3084–3095.
27. Humphrey W, Dalke A, Schulten K. VMD: visual molecular dynamics. *J Mol Graph*. 1996;14:27–38.